JOURNAL OF MATERIALS SCIENCE 31 (1996) 3213–3221

A comparative study of microstructure, mechanical and fracture properties of Ni_3Al-based intermetallics produced by powder metallurgy and standard melting and casting processes

D. BOŽIĆ, N. ILIĆ, M. MITKOV, M. T. JOVANOVIĆ
Institute of Nuclear Science, "Vinča", Materials Science Laboratory, P.O. Box 522, 11001 Belgrade, Yugoslavia

M. ZDUJIĆ
Institute of Technical Science of the Serbian Academy of Science and Arts, Knez Mihailova 35, 11000 Belgrade, Yugoslavia

A comparative study of the microstructure, mechanical properties and fractography of Ni_3Al macro- and microalloyed intermetallics produced by powder metallurgy (PM) and standard vacuum melting and casting processes has been carried out. Non-porous PM compacts were obtained by vacuum hot pressing of powders produced either by gas atomization or by a rotating electrode process. All materials showed a positive temperature dependence of the compression yield strength. The maximum strength was attained between 600 and 700 °C, then the decrease occurs. With increase in temperature the ductility of all materials slightly decreased to a minimum and then abruptly increased. Values of mechanical properties of PM compacts were higher than those of as-cast material. There is a correlation between the fracture morphology and the ductility of Ni_3Al, i.e. the higher ductility corresponds to transgranular fracture, while the minimum ductility is a consequence of intergranular fracture.

1. Introduction

The current interest for the increased efficiency in gas-propulsion systems has invoked a great deal of interest in structural intermetallics, in general, and $L1_2$-based Ni_3Al intermetallic alloys, in particular [1, 2]. The most attractive property of Ni_3Al is that its yield strength increases with increasing temperature from near ambient temperature, to approximately 600 °C [3, 4]. However, polycrystalline Ni_3Al is brittle and undergoes intergranular fracture [5]. The addition of 0.1% B and 8% Cr (at %) [6–9] increases tensile ductility dramatically and promotes transgranular dimple fracture. Nevertheless, superalloys for turbine application have not been replaced by Ni_3Al. The major problem in manufacturing is the strong tendency of aluminium to oxidize at elevated temperature which causes metal–crucible and metal–ceramic interactions during vacuum melting and vacuum investment casting, respectively. One approach is to fabricate the Ni_3Al components in their net shape by powder metallurgy (PM) processes. Many studies of this material have been conducted on hot isostatic pressing (HIP) and hot vacuum pressing (HVP) [10–14]. In addition, PM reduces macro-and micro-segregations, compared to standard melting and casting practice, but it may also lead to grain-boundary embrittlement if the powders were contaminated with oxygen and sulphur [15].

The aim of this paper is to present a comparative study of microstructure, mechanical properties and fracture characteristics of a microalloyed Ni_3Al-based intermetallic produced by PM processes and by standard casting and melting procedure.

2. Experimental procedure

2.1. Material

Boron-doped Ni_3Al (nominal composition (wt %) 12Al–6Fe–1.6Ti–0.15B–balance Ni) has been the object of this study.

The as-cast specimens were vacuum induction melted and poured from about 1480 °C into an Al_2O_3 ceramic mould that was preheated at approximately 800 °C. Ingots were cylinders, 6 mm diameter and 15 mm long.

0022–2461

Powders for PM were produced using two different procedures: (a) gas atomization in an argon atmosphere [16], and (b) the rotating electrode process (REP). The previously cast ingots (25 mm diameter) were *in situ* melted and atomization was performed in the laboratory-designed and constructed apparatus whose principal characteristics are described elsewhere [17]. Helium was used as an inert atmosphere, while melting was realized by an electric arc stabilized by flowing argon. The angular velocity of the rotary electrode was 730 rad s^{-1}.

The time and temperature of vacuum hot pressing were determined by measuring the density of compacts, i.e. the highest density of about 98% was obtained at 1250 °C for 6 h (atomized compacts) and at 1200 °C for 4 h (REP compacts). Compaction pressure was 35 MPa in both cases. All specimens (as-cast and compacts) were machined to final dimensions (6 mm diameter and 12 mm high).

2.2. Testing and characterization

Compressive tests were performed from room temperature to 900 °C in a vacuum at 10^{-1} MPa at a strain rate of 1.3×10^{-3} s^{-1}.

Specimens for optical microscopy were prepared by standard techniques and etched in a solution (vol %) of 25 H_2O, 25 HNO_3, 25 H_3PO_4, 12.5 CH_3COOH and 12.5 HCl.

Energy-dispersive X-ray spectroscopy (EDAX) coupled with the "Philips" scanning electron microscope (SEM) was used for the semiquantitative examination of microstructure. The fracture surface topography was examined by SEM.

3. Results and discussion

3.1. Microstructure

3.1.1. PM compacts

Optical metalography of PM compacts produced by gas atomization and REP is shown in Fig. 1a and b, respectively. The microstructure of PM compacts is homogeneous and non-porous and with an average grain size of 20 μm (for atomized, compacts) and 50 μm (for REP compacts). The grain boundaries of powder particles can be seen in both compacts.

The microstructure of atomized compacts (Fig. 1a) contains relatively large single grains of the individual powder surrounded by small recrystallized grains. These small grains acted as obstacles in preventing grain-boundary movement during hot pressing or annealing treatments. The scanning electron micrograph (Fig. 2a) shows that a "chain" of small particles may be seen at the boundary of prior powder particles. EDAX analysis (Fig. 2b) reveals that these particles are rich in titanium, but the presence of a high peak of sulphur is also observed. Secondary-phase titanium-based particles may also prevent grain-boundary motion. Particles outlining prior powder boundaries (PPB) have been observed in iron-based superalloys produced by PM techniques [18], but in this case a nearly compact film is formed around PPB. Titanium, sulphur, and probably oxygen as TiO_2 [15], affect the formation of

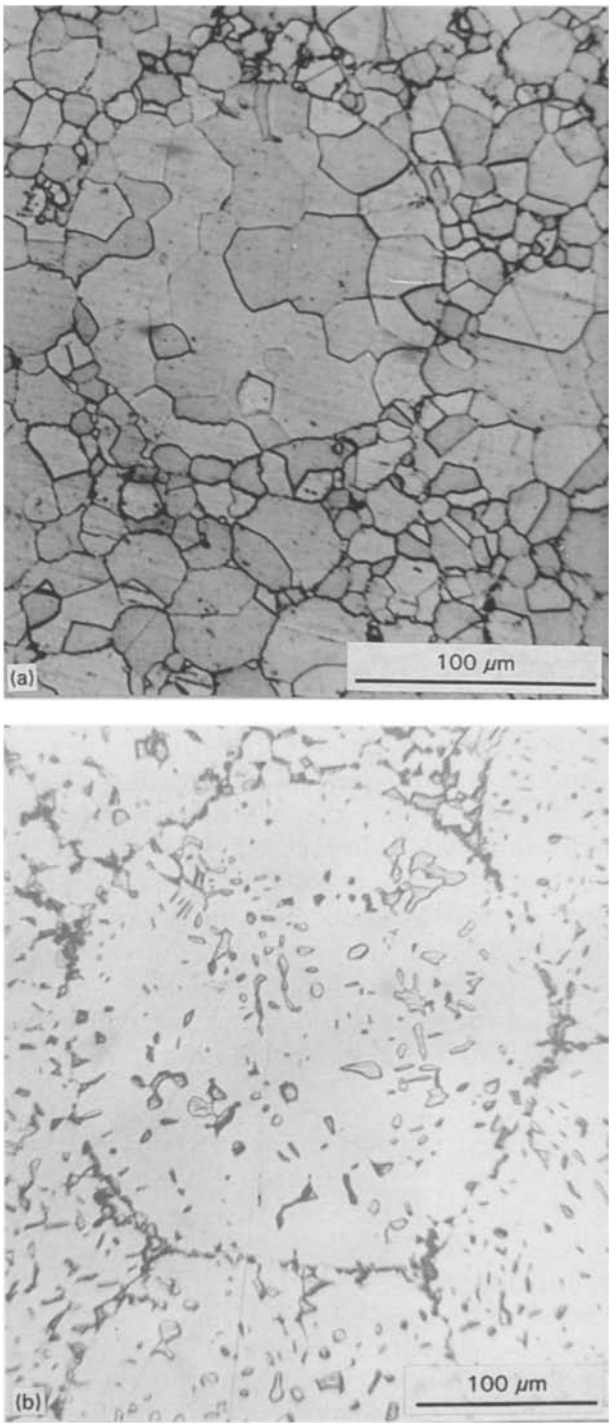

Figure 1 Optical micrographs of (a) atomized and (b) REP PM compact specimens.

that film. On the other side, in the matrix of atomized compacts (Fig. 3a) globular and plate-like particles may be seen. EDAX analysis shows that nickel prevails in the matrix (Fig. 3b), while the particles contain the high amount of titanium and nickel, but the peak corresponding to sulphur is also visible (Fig. 3c). The presence of sulphur in these compacts is probably a consequence of the iron powder being used in the process of gas atomization often being contaminated by sulphur [15]. Generally, these results suggest that atomized compacts are recrystallized fine-grained Ni_3Al material, containing a heterogeneous distribution of very small particles which are mainly located in the intergranular regions representing the prior

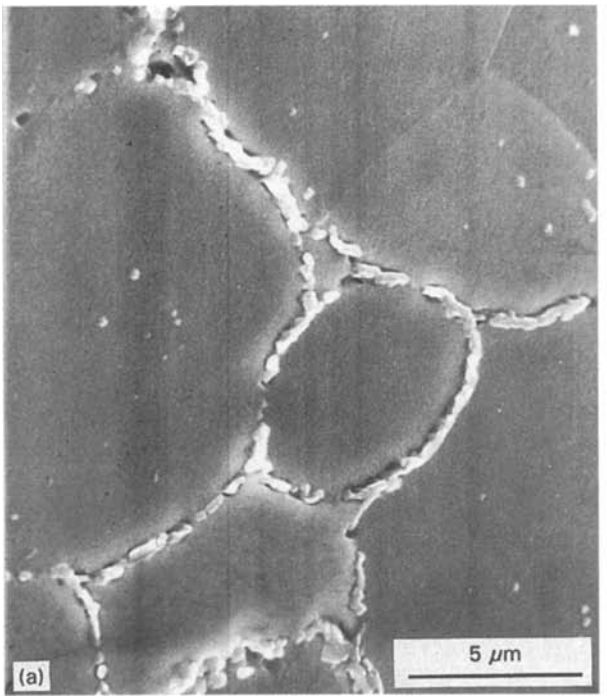

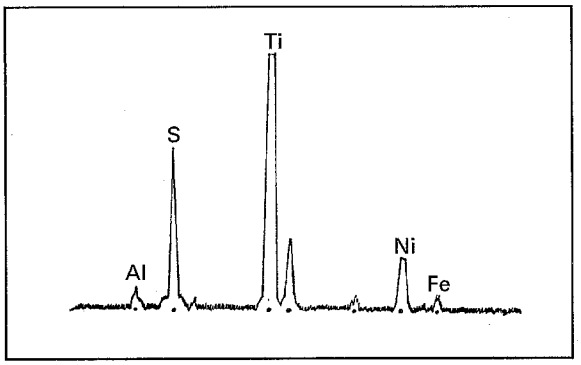

(b)

Figure 2 (a) Scanning electron micrograph and (b) EDAX analysis of prior particle boundaries of atomized PM compact.

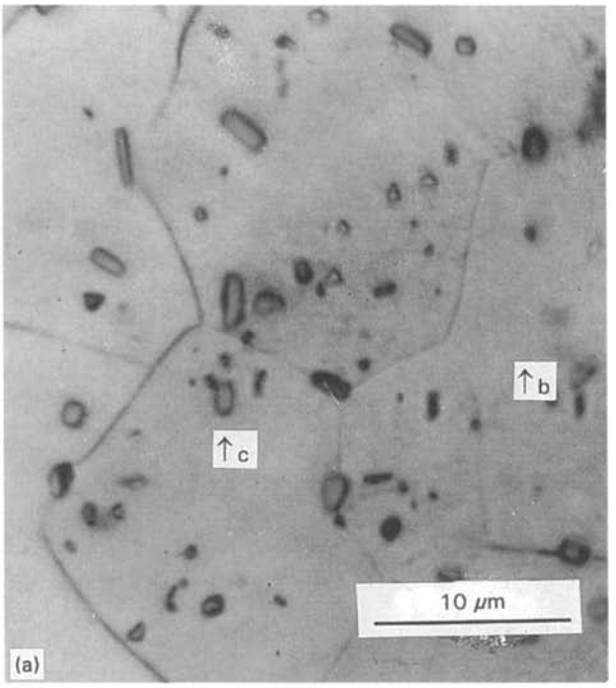

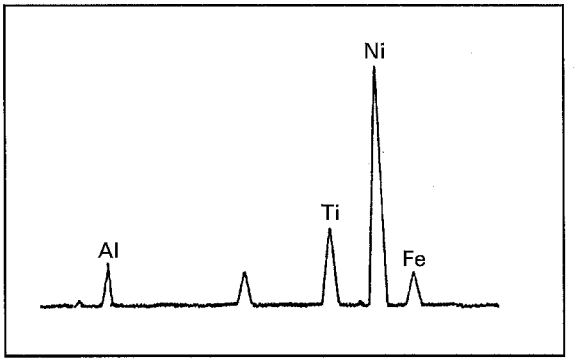

(b)

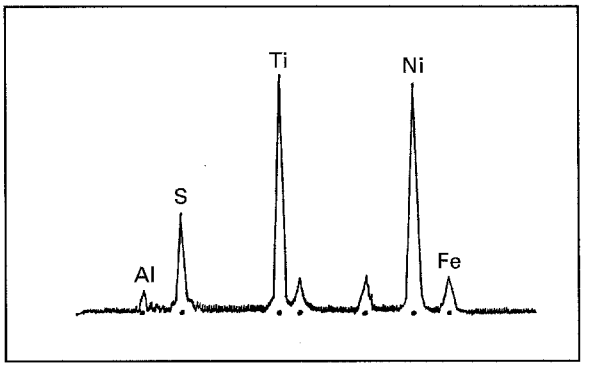

(c)

Figure 3 (a) Optical micrograph and EDAX analysis of (b) the matrix and (c) particles of atomized PM compact.

powder particles. The presence of sulphur was observed in both intergranular regions and in the matrix.

Small particles define the boundaries of former powders of the REP compacts (Fig. 1b). Similar to the atomized compacts, particles of different morphology, i.e. plate-like, globular and polygonal, particles may be seen in the matrix of the REP compacts (Fig. 4a). EDAX analysis shows that nickel is dominant in the matrix and also in globular and polygonal particles (Fig. 4b and d, respectively), while in plate-like particles titanium is a dominant element (Fig. 4c). The higher aluminium content in globular and polygonal particles may imply the presence of NiAl phase. Namely, Laag *et al.* [19] found an amount of NiAl in the matrix of Ni_3Al powders. German [20] claimed that the NiAl phase transforms to Ni_3Al during hot isostatic pressing, but some residual NiAl can be retained. The morphology and chemical composition of the particles in the boundary between previous powders (Fig. 5a) is different from the matrix, i.e. particles of different composition are present: areas rich in Ni + Al and Ni + Ti are observed (Fig. 5b and c, respectively).

The main difference between atomized compacts and REP compacts is the presence of sulphur at the powder particles boundary in the former.

3.1.2. As-cast specimens

The grain size of the as-cast specimens is much larger (approximately 800 μm) than that of PM-processed material (Fig. 6a). Mainly intragranular secondary phase particles may be seen in the micrograph. EDAX analysis shows that nickel strongly prevails in the

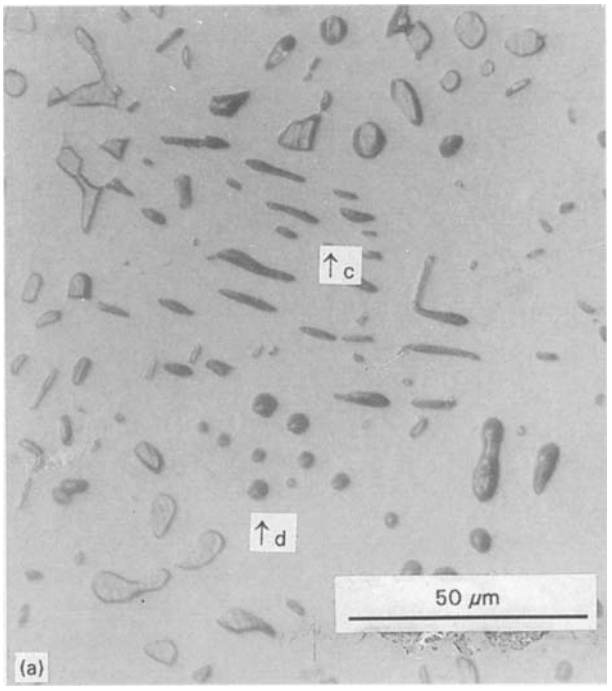

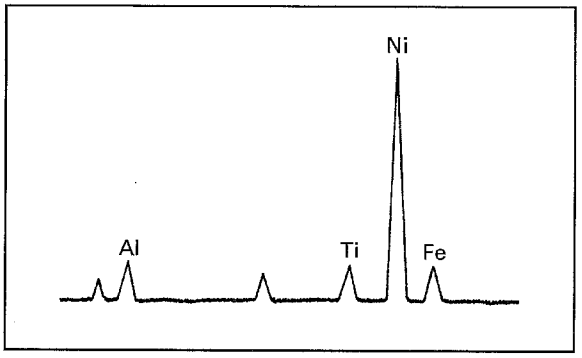

(b)

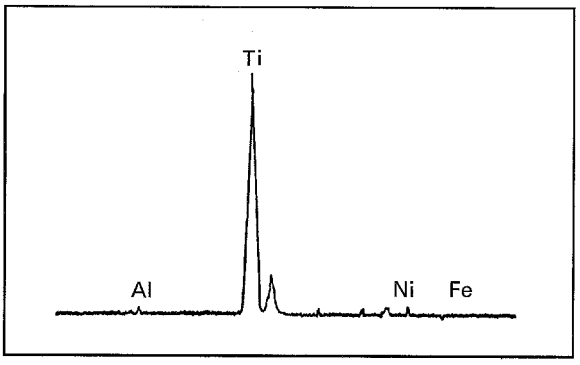

(c)

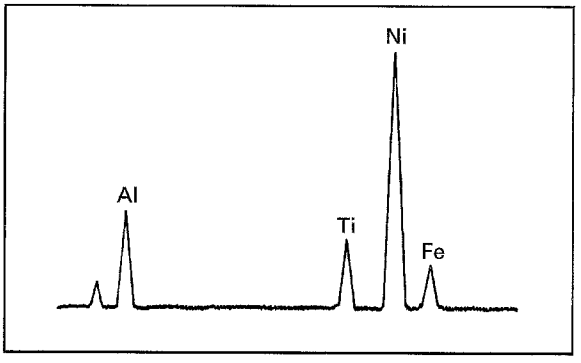

(d)

Figure 4 (a) Optical micrograph and EDAX analysis of (b) the matrix, (c) plate-like particles and (d) globular and polygonal particles of REP PM compact.

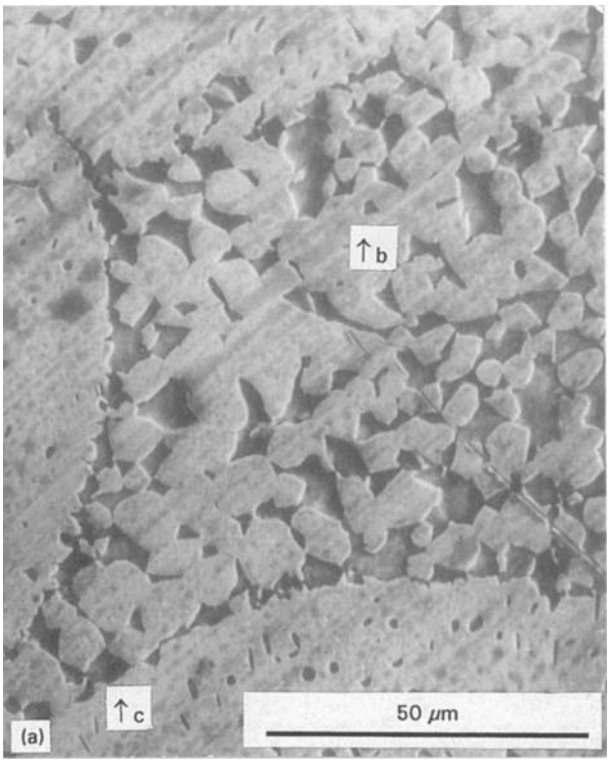

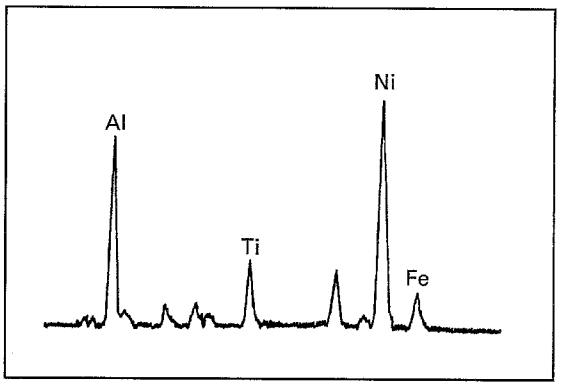

(b)

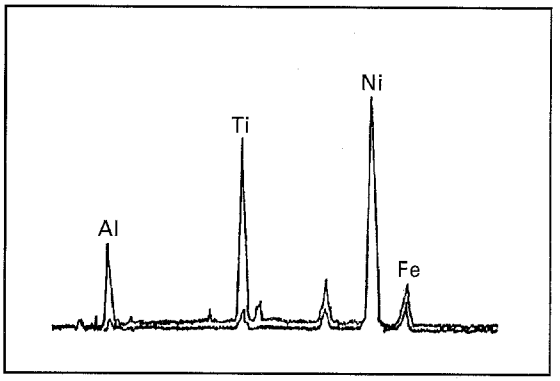

(c)

Figure 5 (a) Scanning electron micrograph and EDAX analysis of the boundary area between previous powders: (b) plate-like particles and (c) globular particles of REP PM compact.

matrix (Fig. 6b), while the amounts of aluminium, titanium and iron are somewhat higher in particles than in the matrix (Fig. 6c).

Summarized results of EDAX analysis showing the distribution of chemical elements in different areas of PM compacts and as-cast specimens, are shown in Table I.

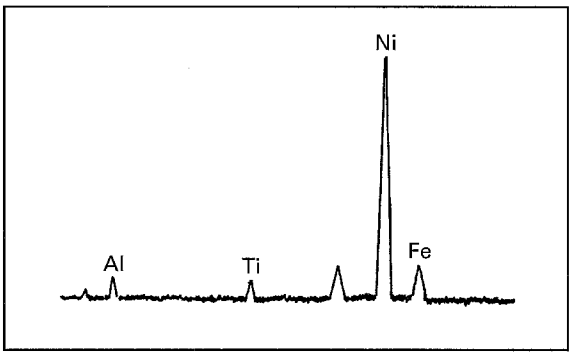

(b)

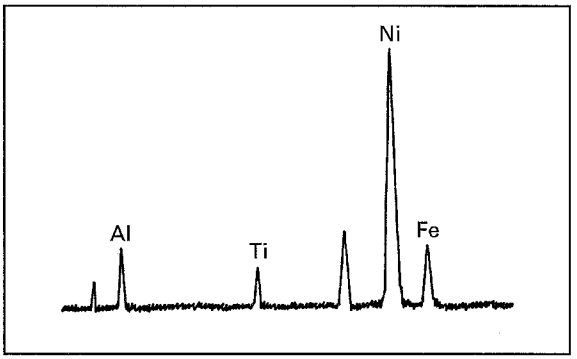

(c)

Figure 6 (a) Light micrograph and EDAX analysis of (b) the matrix and (c) particles of the as-cast specimen.

3.2. Mechanical properties

The effect of temperature on the strength and ductility of the PM and as-cast processed Ni_3Al is shown in Fig. 7a and b, respectively. The yield strength of all materials shows a positive temperature dependence in the range from room temperature to 600–700 °C where the strength peak is reached. The further increase in temperature causes the decrease in strength. PM compacts, as a fine-grained material, exhibit peak strength at somewhat lower temperature (600 °C) than coarse-grained as-cast specimens (700 °C). The strength increases with increase in grain size [21], which is consistent with our results (Fig. 7a) concerning atomized compacts and as-cast specimens. Generally, the finer-grained PM material is stronger than the as-cast material at temperatures below the peak temperature. REP compacts show the highest level of strength.

Over the entire temperature range, the ductility follows the same trend in all specimens, i.e. ductility decreases slightly from room temperature to about 600 °C (as-cast specimens showing the lowest minimum at this temperature) and then abruptly increases as temperature rises. Some literature data [15, 22], however, show that the ductility decrease in the temperature region from room temperature to 700 °C, is more pronounced than in this paper (see Table II). The large increase in ductility at temperatures above 700 °C is in accordance with the previous work [23] which also shows a steep increase in ductility above 800 °C. The ductility results show that the processing technique and grain size have no significant effect on ductility. Actually, the PM material is slightly more ductile than the as-cast material. The lower ductility of atomized compacts (grain size 20 μm) compared to REP compacts (grain size 50 μm) could be ascribed to the amount of sulphur which was found in the matrix and the previous powder particles boundaries.

PM compacts having the finer grain size possess improved mechanical properties compared to as-cast intermetallic alloy. Table II summarizes the yield strength and ductility data of some Ni_3Al based intermetallics produced by PM processes. The values of strength and ductility of atomized compacts and REP compacts are much higher compared to those values from the literature obtained by compressive testing. In both cases one should be cautious when comparing these values and data corresponding to tensile testing.

3.3. Fractography

At room temperature, PM-processed and as-cast material exhibit a transgranular fracture which is mainly ductile and is characterized by microvoid coalescence (Fig. 8). At a temperature corresponding to minimum ductility (600 °C) the fracture mechanism is changed. PM compacts show a transition from predominantly transgranular to predominantly intergranular fracture (Fig. 9a). The diameter of some fractured species corresponds roughly to the grain size of small grains in Fig. 1a. The fracture mechanism of the as-cast material is obviously interdendritic, while some transgranular fracture is also present (Fig. 9b). The ductility is not significantly changed in spite of the change of fracture mechanism. With further increase in temperature, transgranular quasi-cleavage and dimple fracture appear in PM compacts (Fig. 10a), while in the as-cast material transgranular crystallographic fracture prevails (Fig. 10b). Abrupt increase in ductility is probably an indication that the ductile mechanism is fully operative during fracture at high temperatures. However, at 800 °C (REP compacts, only) and 900 °C, PM compacts could not be fractured and barrel-type specimens have been obtained after compressive tests.

TABLE I Summarized EDAX results of elemental distribution in PM compacts and as-cast specimens

Location	PM compacts		As-cast specimens
	Atomized	REP	
Matrix	**Ni**[a], Ti, Al, Fe	**Ni**, Fe, Al, Ti	**Ni**, Fe, Ti, Al
Particles in the matrix			
(a) plate-like	(a, b) **Ti**, **Ni**, S, Fe, Al	(a) **Ti**, Al	(a) **Ni**, Fe, Ti, Al
(b) globular			
(c) polygonal		(b, c) **Ni**, Al, Fe	
Particles in the boundary between powder surfaces	**Ti**, S, Ni, Al, Fe	**Ni**, **Al**, Ti, Fe (plate-like) **Ni**, **Ti**, Al, Fe (globular)	

[a] The sequence of elements is arranged according to their EDAX peak heights. Bold-printed elements show the highest peak.

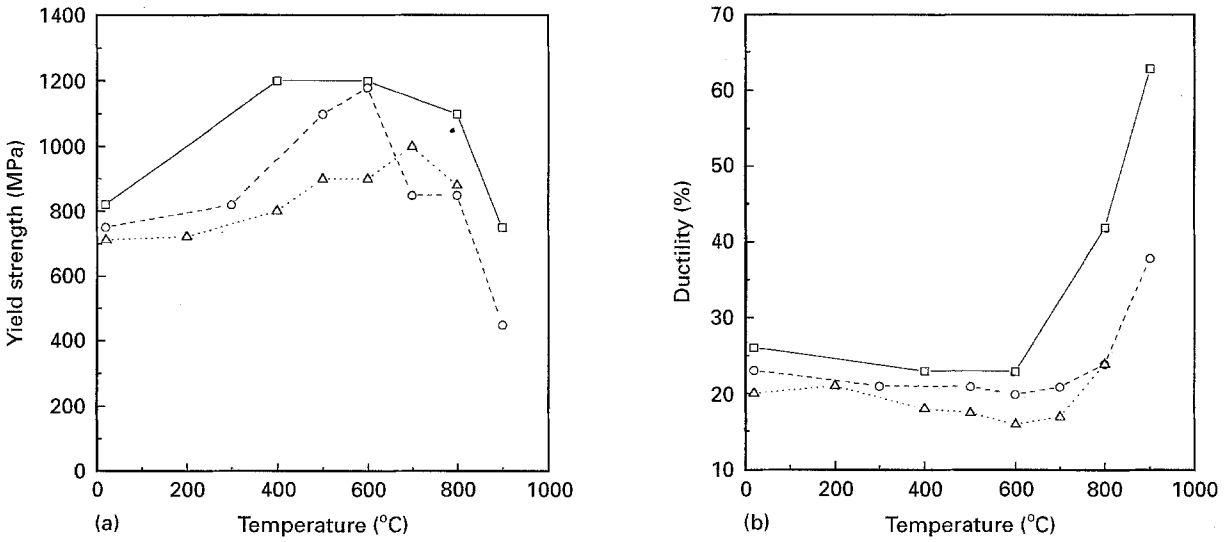

Figure 7 The effect of temperature on (a) the compressive yield stress and (b) ductility of PM compacts and as-cast Ni_3Al-based intermetallics. (–□–) REP compacts (PM), (–○–) atomized compacts (PM), (·· △ ··) as-cast specimens.

TABLE II Yield strength, $\sigma_{0.2}$, and ductility, ε, for various Ni_3Al-based intermetallics obtained through powder metallurgy processes

Composition	Mode of compaction[a]	Grain size (μm)	Temp. (°C)	$\sigma_{0.2}$ (MPa)	ε (%)	Reference
Ni_3Al–B	HIP	40	R.t.	350	28	
			600	450		[15]
			700	–	2	
Ni_3Al–Cr–B	HIP	35	R.t.	530	34	
			600	650	–	[15]
			700	–	2	
Ni_3Al–Cr–B	HE	15	R.t.	650	40	
			600	720	–	[15]
			700	–	7	
Ni_3Al–Hf–B	HE	1.9	R.t.	727	30.2	
		32	R.t.	319	47.2	[24]
Ni_3Al–B	HE	30	R.t.[b]	300	10	
			600[b]	580	–	[22]
			700	–	4	
75% Ni_3Al–Cr–Si–B			R.t.	600	34	
+	HE	–	700	680	1	[24]
25% Ni_3Si						
Ni_3Al	RS	24	R.t.	410	19	[25]
Ni_3Al–B	HE	40	R.t.[b]	420	–	
			600[b]	850	–	[26]
Ni_3Al–B	HE	40	R.t.[b]	1100	15	
			550	1100	18	[27]
Ni_3Al–Ti–Fe–B	HVP	50	R.t.[b]	820	26	This
			600[b]	1200	23	work
Ni_3Al–Ti–Fe–B	HVP	20	R.t.[b]	750	23	This
(atomized			600[b]	1180	20	work
compacts)						

[a] HIP, hot isostatic pressing; HE, hot extrusion; RS, reactive synthesis; HVP, hot vacuum pressing, Rt, room temperature.
[b] Compression testing.

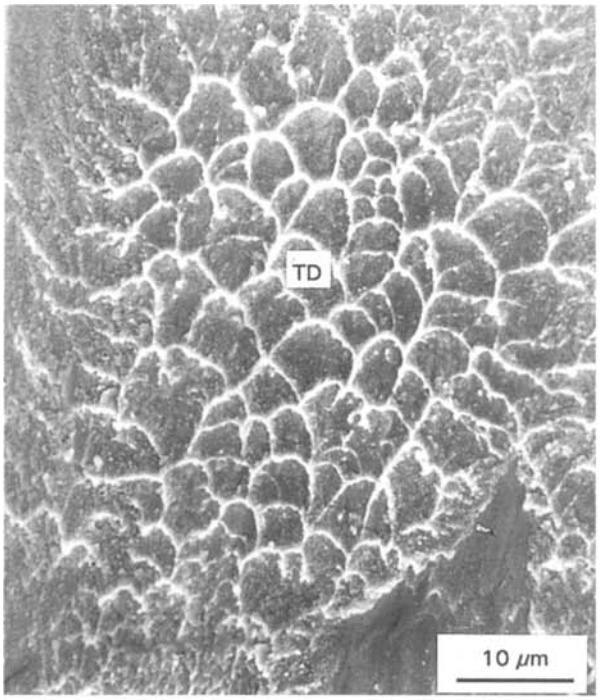

Figure 8 SEM microfractograph of atomized PM compact room temperature. TD, transgranular dimples.

The minimum ductility corresponds to intergranular fracture, and the amount of this fracture is higher in PM compacts. However, it was not possible to correlate the intergranular mode of fracture to the presence of sulphur on the surface of atomized powders, or, the influence of particles in the grain-boundary area (Fig. 5a) on the ductility of REP compacts. Although there is a correlation between the fracture mode and ductility, the latter is slightly affected by fracture in the range from room temperature to 700 °C. There is no evidence of the mechanism involved in fracture at 800 and 900 °C when the highest values of ductility (PM compacts) have been reached.

4. Conclusions

1. All materials exhibit a positive temperature dependence of the compression yield strength. The maximum yield strength is between 600 and 700 °C, then a decrease occurs. PM compacts prepared by the REP process show the highest strength (about 1200 MPa at 700 °C).

2. The ductility of all materials slightly decreases from room temperature to 600 °C, then steeply increases with further increase in temperature.

3. Mechanical properties (especially strength) of PM compacts are superior to those of as-cast material.

4. A correlation between ductility and the fracture mode exists for all materials: the minimum ductility always corresponds to intergranular fracture, while the higher ductility is ascribed to transgranular fracture.

Acknowledgement

This research was financially supported by the Scientific Research Fund of Serbia.

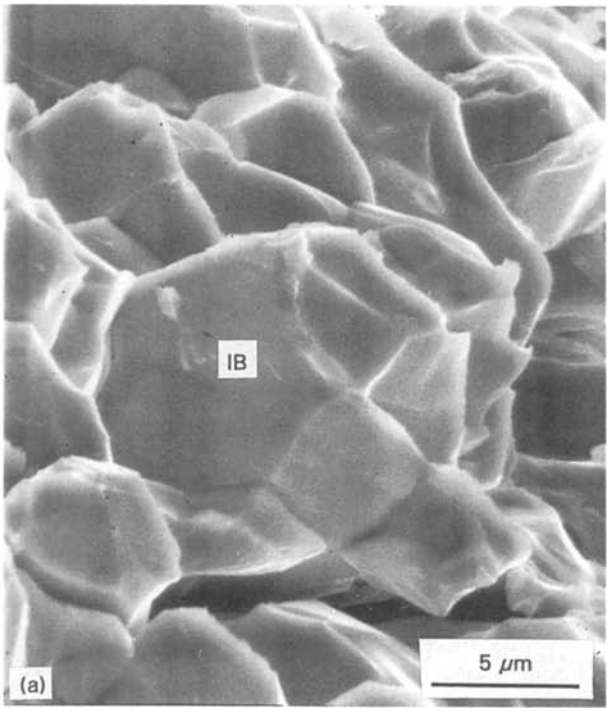

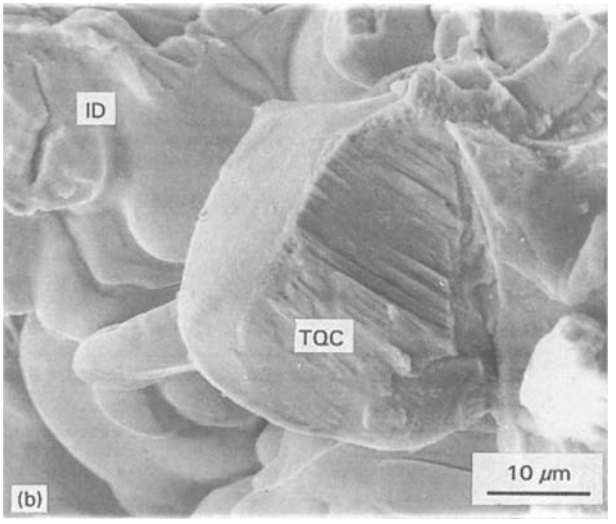

Figure 9 SEM microfractographs of (a) atomized PM compact and (b) as-cast specimen at 600 °C. Note the wide secondary crack in (a). IB, intergranular brittle fracture; ID, interdendritic brittle fracture; TQC, quasi-cleavage transgranular fracture.

Appendix. Determination of the cooling rate of a metal droplet

Theoretical calculation of cooling rate

The values of the physical properties and constants used in the calculations are given in Table III.

The heat-transfer coefficient from the metal droplet to the surrounding gas is defined by the dimensionless Nusselt's number:

$$\mathrm{Nu} = hd/\lambda_g \qquad \text{(A1)}$$

where h is the heat transfer coefficient ($\mathrm{W\,m^{-2}\,K^{-1}}$); d the particle (droplet) diameter (m) and λ_g is the thermal conductivity of gas ($\mathrm{W\,m^{-1}\,K^{-1}}$).

When the heat transfer is pure conduction, then Nu = 2, giving the possibility of calculating the lowest value of the heat-transfer coefficient, h. When the heat

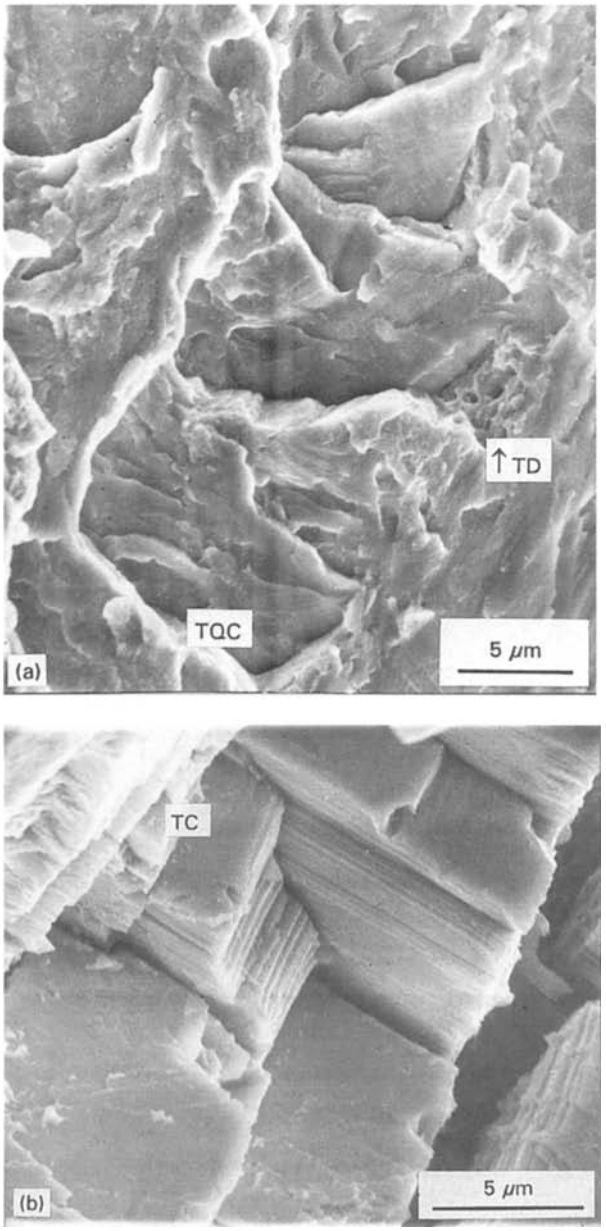

Figure 10 SEM microfractograph of (a) REP PM compact and (b) as-cast specimen at 800 °C. TD, transgranular dimples; TQC, quasi-cleavage transgranular fracture; TC, transgranular crystallographic fracture.

is transferred by radiation and convention, h may be derived from the equation

$$\mathrm{Nu} = 2 + 0.6\mathrm{Pr}^{1/3}\mathrm{Re}^{1/2} \quad \text{(A2)}$$

where $\mathrm{Pr} = C_{pg}\mu_g/\lambda_g$ and $\mathrm{Re} = d\rho_g u/\mu_g$ while u is the particle velocity (ms^{-1}).

The cooling rate in the case of heat transfer by radiation and convection is given by

$$dT/dt = \frac{6h(T_s - T_g) + 6\,\varepsilon\sigma_v(T_s^4 - T_w^4)}{C_p\,\rho\,d} \quad \text{(A3)}$$

where dT/dt is the cooling rate ($\mathrm{K\,s}^{-1}$), T_s is the temperature of metal (K), T_g is the temperature of the gas (K), σv the Stephan–Boltzman constant ($5.7 \times 10^{-8}\ \mathrm{W\,m}^{-2}\,\mathrm{K}^{-4}$).

From Equation A_3 and considering that the average diameters of powders are 70 μm (gas atomization) and 360 μm (REP), the cooling rates of droplets during powder production have been extrapolated from Fig. A1.

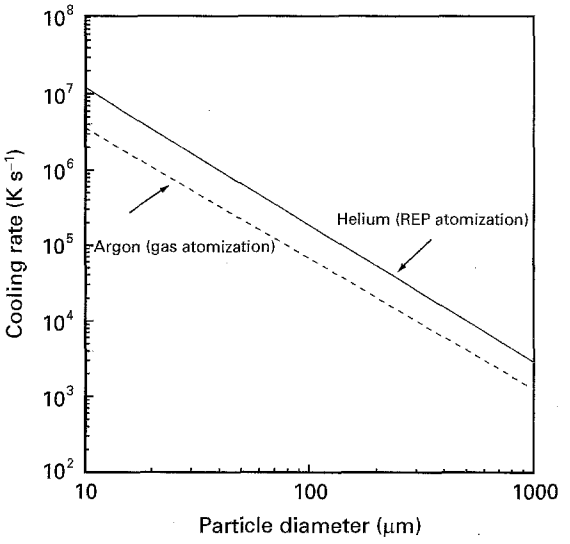

Figure A1 Variation of particle radius with cooling rate of argon-atomized and REP powders.

TABLE III Physical properties and constants used in calculations

Ni_3Al		
Melting point, T_m	1663 K	
Density, ρ	7500 kg m^{-3} (solid Ni_3Al)	
Specific heat, C_p	656 $J\,kg^{-1}\,K^{-1}$ (liquid nickel)	
Emissivity	0.25	
Gaseous properties	Argon	Helium
Temperature of surrounding gas, T_g (K)	323	323
Film temperature, $T_f = 1/2\ (T_s + T_g)$ (K)	993	993
Thermal conductivity at T_f, λ_f ($\mathrm{W\,m}^{-1}\,\mathrm{K}^{-1}$)	0.453	0.352
Viscosity of T_f, μ_f (Pa s)	5.33×10^{-5}	4.41×10^{-5}
Specific heat, C_{pg} ($\mathrm{J\,mol}^{-1}\cdot\mathrm{K}^{-1}$)	20.81	20.81
Molar weight, M_g ($\mathrm{kg\,mol}^{-1}$)	39.948×10^{-3}	4.0026×10^{-3}
Density at T_g and ρ = 0.1 MPa, ρ_g ($\mathrm{kg\,m}^{-3}$)	1.488	0.149

References

1. N. S. STOLOFF, *Int. Met. Rev.* **29** (1984) 123.
2. C. T. LIU, in Proceedings of the Conference, "High Temperature Ordered Intermetallic Alloys IV", edited by L. A. Johnson, D. P. Pope and J. D. Stiegler (Materials Research Society Proceedings, Materials Research Society, Pittsburgh, PA, 1991) Vol. 213, p. 168.
3. F. H. THORNTON, R. C. DAVIES and T. L. JOHNSTON, *Metall. Trans.* **1** (1970) 207.
4. N. S. STOLOFF and R. C. DAVIES, *Prog. Mater. Sci.* **13** (1968) 3.
5. C. T. LIU, in Proceedings of the Conference, "High Temperature Ordered Intermetallic Alloys II", edited by N. S. Stoloff, C. C. Koch, C. T. Liu and O. Izumi (Materials Research Society Proceedings, Materials Research Society, Pittsburgh, PA, 1987) Vol. 81.
6. K. AOKI and O. IZUMI, *Nippon Kinzako Gakkaishi* **43** (1979) 1190.
7. A. I. TAUB, S. C. HUANG and M. K. CHANG, *Metall. Trans.* **15A** (1984) 399.
8. C. T. LIU and V. K. SIKKA, *J. Metals* **36** (1986) 19.
9. C. T. LIU, C. L. WHITE and J. A. HORTON, *Acta Metall.* **33** (1985) 213.
10. A. BOSE, B. MOORE, R. M. GERMAN and N. S. STOLOFF, *J. Metals* September (1988) 14.
11. A. BOSE, B. H. RABIN and R. M. GERMAN, *Powder Metall. Int.* **20** (3) (1988) 25.
12. C. NISHIMURA and C. T. LIU, *Scripta Metall.* **26** (1992) 381.
13. M. JOVANOVIĆ, D. BOŽIĆ, N. ILIĆ, Đ. DROBNJAK and M. MITKOV, *Mat. Charact.* **32** (1994) 89.
14. D. BOŽIĆ, M. MITKOV, N. ILIĆ, M. T. JOVANOVIĆ and M. ZDUJIĆ, *Mater. Lett.* **21** (1994) 161.
15. R. N. WRIGHT and J. E. FLINN, in Proceedings of the Conference, "Hot Isostatic Pressing", edited by T. Garvare (Centek Publishing, Lulea, Sweden 1988) p. 225.
16. D. BOŽIĆ, M. MITKOV, N. ILIĆ, M. T. JOVANOVIĆ, *Sci. Sint.* **24** (1992) 191.
17. M. ZDUJIĆ, M. SOKIĆ, V. PETROVIĆ and D. USKOKOVIĆ, *Powder. Metall. Int.* **18** (1986) 275.
18. G. H. GESSINGER, "Powder Metallurgy of Superalloys" (Butterworth, New York, 1981) p. 101.
19. R. LAAG, V. TAFNER, W. A. KAYSSER and G. PETZOW, *Prakt. Metall.* **26** (1989) 404.
20. R. M. GERMAN, in Proceedings of the Conference, "Sintering' 89", edited by D. P. Uskoković, H. Palmour III and R. M. Spriggs (Plenum, New York, 1987) p. 439.
21. M. TAKEYAMA and C. T. LIU, *Acta Metall.* **36** (1988) 1241.
22. T. P. WEIGHS, V. ZINOVIEV, V. D. VIENS and E. M. SCHULSON, *ibid.* **35** (1987) 1109.
23. V. K. SIKKA and E. A. LORIA, in Proceedings of the Conference, "Superalloys 1988", edited by M. Gell and J. Radavitch (The Metallurgical Society, Seven Springs, 1988) p. 48.
24. P. S. KHADIKAR, K. VEDULA and B. S. SHABEL, *Metall. Trans.* **18A** (1987) 425.
25. A. V. BASE and V. K. SIKKA, in Proceedings of the Conference "Speciality Materials and Composites", edited by A. Lawley and A. Swanson (American Powder Metallurgy Institute, Princeton, NJ, 1993) p. 15.
26. R. M. COOPER, K. SHAW, K. McCOY, R. M. GERMAN and L. SMITH, *ibid.* p. 53.
27. H. V. SIZEK and G. T. GRAY III, *Acta Metall.* **41** (1993) 1855.

Received 25 April 1995
and accepted 23 November 1995